

An Improved Non-Iterative Surface Layer Flux Scheme for Atmospheric Stable Stratification Condition

Y. Li^{1,2,3}, Z. Gao^{1,2}, D. Li⁴, L. Wang², and H. Wang¹

[1]{Jiangsu Key Laboratory of Agriculture Meteorology, Collaborative Innovation Center on Forecast and Evaluation of Meteorological Disasters, College of Applied Meteorology, Nanjing University of Information Science and Technology, Nanjing, Jiangsu, China}

[2]{State Key Laboratory of Atmospheric Boundary Layer Physics and Atmospheric Chemistry, Institute of Atmospheric Physics, Chinese Academy of Sciences, Beijing, China}

[3]{School of Energy and Environment, Guy Carpenter Asia-Pacific Climate Impact Centre, City University of Hong Kong, Hong Kong, China}

[4]{Program of Atmospheric and Oceanic Sciences, Princeton University, Princeton, NJ 08540, USA}

Correspondence to: Z. Gao (zgao@mail.iap.ac.cn)

Abstract

Parameterization of turbulent fluxes under stably stratified conditions has always been a challenge. Current surface fluxes calculation schemes either need iterations or suffer low accuracy. In this paper, a non-iteration scheme is proposed to approach the classic iterative computation results using multiple regressions. It can be applied to the full range of roughness status $10 \leq z / z_0 \leq 10^5$ and $-0.5 \leq \log(z_0 / z_{0h}) \leq 30$ under stable conditions $0 < Ri_B \leq 2.5$. The maximum (average) relative errors for the turbulent transfer coefficients for momentum and sensible heat are 12% (1%) and 9% (1%), respectively.

1 Introduction

In weather or climate models, the earth's surface is the boundary that needs to be resolved physically (Chen and Dudhia, 2001). The condition of atmosphere aloft (e.g., wind, temperature and humidity) is highly dependent on the momentum, sensible heat and latent heat fluxes at surface. Currently, the exchanges of momentum and heat between the earth's surface and the

atmosphere are usually calculated with various schemes based on Monin-Obukhov similarity theory (hereinafter MOST, Monin and Obukhov, 1954) in models. These schemes (e.g., Paulson, 1970; Businger, 1971; Dyer 1974; Holtslag and De Bruin, 1988, Beljaars and Holtslag, 1991; Janjić 1994; Launiainen, 1995; Högström, 1996) are similar to each other but the differences among them exist due to different observational data and/or mathematical solutions that were used in retrieving the schemes. One commonly used scheme is Businger-Dyer (BD) equation (Businger, 1966; Dyer, 1967). However, the BD equation suppresses fluxes under stable condition too quickly and is not applicable when the Richardson number exceeds a critical value (Louis, 1979). Holtslag and De Bruin (1988) and Beljaars and Holtslag (1991) proposed alternative schemes which can be used under very stable conditions. With data collected in the field program CASES-99 (Cooperative Atmosphere-Surface Exchange Study-99) (Poulos et al., 2002), Cheng and Brutsaert (2005, CB05 hereinafter) further provided a new scheme and it is confirmed to perform better by later research (Guo and Zhang, 2007; Jiménez et al, 2012). Based on the measurements made during experiment SHEBA in Arctic and Halley 2003 experiment in Antarctica, Grachev et al. (2007) and Sanz Rodrigo and Anderson (2013) proposed different similarity functions, respectively. Through systematic mathematical analysis, Sharan and Kumar (2011) proved that similarity functions of CB05 and Grachev et al. (2007) were applicable in the whole stable stratification region. However, all of these studies are based on MOST and application of MOST in very stable condition is in doubt since it assumes that turbulence is continuous and stationary, while in very stable condition turbulence is weak, sporadic and patchy (Sharan and Kumar, 2011). Grachev et al. (2013) indicates that the applicability of local MOST in stable conditions is limited by the inequalities, when both gradient and flux Richardson numbers are below their "critical values" about 0.20-0.25. Further, MOST predicts that mean gradients of turbulence become independent of z in very stable condition, Wyngaard and Coté (1972) first referred to this limit as 'z-less stratification'. BD equations follow this prediction, but CB05 and Grachev et al. (2007) do not. To avoid these holdbacks and self-correlation of MOST, Sorbjan (2010) and Sorbjan and Grachev (2010) discussed an alternative local scaling for the stable boundary layer (referred to as gradient-based scaling) when different universal functions plotted versus the gradient Richardson number instead of the Monin-Obukhov stability parameter.

Another critical issue regarding the fluxes calculation with MOST is the numerical iteration. Under unstable condition, the iteration normally converges within 5 steps (Fairall et al, 1996). By taking advantage of a bulk Richardson number parameterization for an improved first guess

(Grachev and Fairall, 1997), the iteration can be reduced to 3 steps (Fairall et al, 2003). In the Weather Research Forecasting (WRF) model (Skamarock et al., 2008) MM5 similarity surface module, the flux variables from the previous time step are used to calculate the fluxes at current time step and such an approach can yield reasonable result (Jiménez et al, 2012). On the other hand, under stable condition, the flux calculation takes many more steps to converge and hence is time consuming. To avoid the iteration process, a series of non-iterative schemes are proposed (e.g., Loius, 1979, Garratt, 1992, Launiainen, 1995, Song, 1998, De Bruinet al. 2000, Yang et al., 2001; Li et al., 2010), but they all fail to cover the full range of $-0.5 \leq kB^{-1} \leq 30$, $10 \leq z/z_0 \leq 10^5$ and $-5.0 \leq Ri_B \leq 2.5$, which is pointed out by Wouters et al. (2012, WRL12 hereinafter). Here $kB^{-1} = \ln(z_0/z_{0h})$. z is the reference height; and z_0 and z_{0h} are the aerodynamic and thermal roughness lengths, respectively. Ri_B is the bulk Richardson number. Following WRL12, the condition that $Ri_B > 2.5$ is not considered in this study, because it represents extremely stable stratification with very weak wind and little flux exchange. To calculate fluxes under all conditions, and also to include the roughness sublayer effect, WRL12 proposed an updated scheme based on the iterated results of CB05 under stable condition. However, for a given Ri_B , WRL12 uses only one equation to cover the whole large range of z/z_0 and kB^{-1} , which results in biases at some z/z_0 and kB^{-1} conditions. Therefore, to avoid the iteration process and keep the accuracy at the same time, the objective of this paper is to propose a group of equations that divide the calculation into 8 regions according to z_0 and z_{0h} values. To compare with WRL12, and with the fact that CB05 equations are currently widely accepted, the new equations are also based on the iterated results of CB05 equations. Section 2 describes the calculation results from CB05 and WRL12. Section 3 introduces the new equations, and section 4 intercompares these schemes. Summary and conclusions are presented in section 5

2 Revisiting CB05 and WRL12

The momentum flux τ and sensible heat flux H are defined as:

$$\tau \equiv \rho u_*^2 \quad (1)$$

$$H \equiv -\rho c_p u_* \theta_* \quad (2)$$

1 Here u_* is the friction velocity, θ_* is the temperature scale, ρ the air density and c_p the
 2 specific heat capacity at constant pressure. Based on MOST, the friction velocity u_* and
 3 temperature scale θ_* can be calculated by:

$$4 \quad u_* = uk / [\ln(\frac{z}{z_0}) - \psi_m(\frac{z}{L}) + \psi_m(\frac{z_0}{L}) + \psi_m^*(\frac{z}{L}, \frac{z}{z_*})] \quad (3)$$

$$5 \quad \theta_* = (\theta - \theta_0)k / [\ln(\frac{z}{z_{0h}}) - \psi_h(\frac{z}{L}) + \psi_h(\frac{z_{0h}}{L}) + \psi_h^*(\frac{z}{L}, \frac{z}{z_*})] \quad (4)$$

6 Here u and θ are the wind speed and potential temperature at the reference height z . k is the
 7 von Karman constant. z_* is the roughness sublayer height. θ_0 is the potential temperature at the
 8 height of z_{0h} . ψ_m and ψ_h are the integrated stability functions for momentum and heat,
 9 respectively. ψ_m^* and ψ_h^* are the correction functions [accounting for](#) roughness sublayer effect.
 10 L is the Obukhov length defined as:

$$11 \quad L \equiv u_*^2 \bar{\theta} / (kg\theta_*) \quad (5)$$

12 ψ_m^* and ψ_h^* are given by De Ridder (2010):

$$13 \quad \psi_{m,h}^*(\frac{z}{L}, \frac{z}{z_*}) = \int_z^\infty \frac{\phi_{m,h}(\frac{z'}{L})}{z'} e^{-\mu_{m,h} \frac{z'}{z_*}} dz' \quad (6)$$

14 $\mu_m = 2.59$, $\mu_h = 0.95$, and $\phi_{m,h}$ are the stability functions for momentum and heat. Following
 15 Sarkar and De Ridder (2010) and WRL12, $z_*/z_0 = 16.7$ is adopted in this study.

16 CB05 gives the form of $\phi_{m,h}$ and $\psi_{m,h}$:

$$17 \quad \phi_m = 1 + a \frac{\zeta + \zeta^b (1 + \zeta^b)^{\frac{1-b}{b}}}{\zeta + (1 + \zeta^b)^{\frac{1}{b}}} \quad (7)$$

$$18 \quad \phi_h = 1 + c \frac{\zeta + \zeta^d (1 + \zeta^d)^{\frac{1-d}{d}}}{\zeta + (1 + \zeta^d)^{\frac{1}{d}}} \quad (8)$$

$$19 \quad \psi_m = -a \ln(\zeta + (1 + \zeta^b)^{\frac{1}{b}}) \quad (9)$$

$$\psi_h = -c \ln(\zeta + (1 + \zeta^d)^{\frac{1}{d}}) \quad (10)$$

Here $a = 6.1, b = 2.5, c = 5.3$ and $d = 1.1$. $\zeta \equiv z/L$ is the stability parameter.

With Eqs. (3), (4), (5), and (6), $\phi_{m,h}$ and $\psi_{m,h}$ of CB05, fluxes can be calculated through iterations: with a first guess of ζ , u_* and θ_* can be calculated from Eqs. (3) and (4), then ζ again can be derived from Eq. (5). This procedure iterates until the results converge. The relationships of $\zeta \sim Ri_B$, $\zeta \sim \ln(z/z_0)$, and $\zeta \sim \ln(z_0/z_{0h})$ from CB05 are shown in Fig. 1, Fig. 2 and Fig. 3, respectively. **Conditions with $Ri_B = 0.05, 0.2, 0.5$, $z/z_0 = 10, 1000, 10^5$ and $kB^{-1} = -0.5, 15, 30$ are plotted.** However, due to the limitation of computational time in numerical weather and climate models, the calculation results after 5 steps are always taken to approximate the fluxes (e.g., MYJ and MYNN surface module in WRF model, Janjić, 1996, Nakanishi M, Niino, 2006). It is found that with the first guess of $\zeta_0 = Ri_B \frac{[\ln(z/z_0)]^2}{\ln(z/z_{0h})}$ and 5 steps of iteration, the results are still far away from the precise value. **Fig. 4 presents the relative error $\Delta\zeta$ for various Ri_B with $z/z_0 = 10, 1000, 10^5$ and $kB^{-1} = -0.5, 15, 30$.** The relative error $\Delta\zeta$ that is calculated by Eq. 11 can exceed 70% under certain conditions.

$$\Delta\zeta = \begin{cases} \frac{|\zeta_{(cal)} - \zeta_{(precise)}|}{\zeta_{(precise)}} \times 100\%, & \text{for } |\zeta_{(cal)} - \zeta_{(precise)}| \geq 0.01 \\ 0, & \text{for } |\zeta_{(cal)} - \zeta_{(precise)}| < 0.01 \end{cases} \quad (11)$$

where $\zeta_{(cal)}$ is the calculation result, and $\zeta_{(precise)}$ is the precise result from the ultimate iteration of CB05 (when $|\zeta_{(n+1)} - \zeta_{(n)}| < 0.1\% \zeta_{(n)}$, $\zeta_{(n)}$ is adopted as $\zeta_{(precise)}$, and here n indicates the iteration step). **Fig. 5 shows the steps needed to converge into 5% relative error with CB05 equations for various Ri_B with $z/z_0 = 10, 1000, 10^5$ and $kB^{-1} = -0.5, 15, 30$. It shows that when $Ri_B = 0.74$, $z/z_0 = 10$ and $kB^{-1} = 30$, more than 80 steps of iteration are needed to reduce the calculation error within 5%. The iteration takes more steps to converge when there is a larger aerodynamic roughness length z_0 and a smaller thermal roughness length z_{0h} , which is common over an urban surface (Sugawara and Narita, 2009). When $z/z_0 = 10$ and $kB^{-1} = 30$, the largest error can reach 75% after 5 steps iteration (Fig. 4) and 82 steps are needed for the results to converge (Fig. 5). However, when z/z_0 becomes large, for example $z/z_0 = 10^5$ (i.e.,**

a representative value for a smooth sea surface), 5 steps are enough for the results to be within 5% error under all kB^{-1} and Ri_B conditions (Fig. 5).

To avoid the iteration, and based on CB05's iteration results, WRL12 proposed the following set of equations:

$$\zeta_t = -0.316 - 0.515e^{-L_{0H}} + 25.8e^{-2L_{0H}} + 4.36L_{0H}^{-1} - 6.39L_{0H}^{-2} + 0.834\log(L_{0M}) - 0.0267\log^2(L_{0M}), \quad (12)$$

$$Ri_{B,t} = \zeta_t \frac{L_{0H}^* + S_{0H}^* \beta_H \zeta_t}{(L_{0M}^* + S_{0M}^* \beta_M \zeta_t)^2}, \quad (13)$$

$$\zeta = \frac{-L_{0M}^*}{S_{0M}^* \beta_M} - \frac{BC}{4(S_{0M}^* \beta_M)^3 (B^2 + |Cr|)} + \frac{B - \sqrt{B^2 + Cr} + \frac{BCr}{2(B^2 + |Cr|)}}{2(S_{0M}^* \beta_M)^3 r}, \quad (\text{for } Ri_B \leq Ri_{B,t}), \quad (14)$$

$$\zeta = \zeta_t + D(\zeta_t)(Ri_B - Ri_{B,t}), \quad (\text{for } Ri_B > Ri_{B,t}), \quad (15)$$

$$D(\zeta_t) = \frac{(L_{0M}^* + S_{0M}^* \beta_M \zeta_t)^3}{L_{0M}^* L_{0H}^* + \zeta_t (2S_{0H}^* \beta_H L_{0M}^* - S_{0M}^* \beta_M L_{0H}^*)}, \quad (16)$$

where

$$L_{0i} = \ln(z / z_{0i}), \quad (i \text{ stands for M or H}), \quad (17)$$

$$L_{0i}^* = L_{0i} + \frac{1}{\lambda} \ln\left(1 + \frac{\lambda}{\mu_i \frac{z}{z_*}}\right) e^{-\mu_i \frac{z}{z_*}}, \quad (i \text{ stands for M or H}), \quad (18)$$

$$r = Ri_B - S_{0H}^* \beta_H / (S_{0M}^* \beta_M)^2 \quad (19)$$

$$B = S_{0M}^* \beta_M L_{0H}^* - 2S_{0H}^* \beta_H L_{0M}^* \quad (20)$$

$$C = 4(S_{0M}^* \beta_M)^2 L_{0M}^* (S_{0H}^* \beta_H L_{0M}^* - S_{0M}^* \beta_M L_{0H}^*) \quad (21)$$

$$S_{0i}^* = 1 - z_{0i} / z + \left(1 + \frac{\nu}{\mu_i \frac{z}{z_*}}\right) \frac{1}{\lambda} \ln\left(1 + \frac{\lambda}{\mu_i \frac{z}{z_*}}\right) e^{-\mu_i \frac{z}{z_*}} \quad (22)$$

where $\lambda = 1.5$, $\nu = 0.5$, $\beta_M = 4.76 + 7.03z_0 / z + 0.24z_{0h} / z_0$ and $\beta_H = 5$. First, $Ri_{B,t}$ is calculated from Eqs. (12) and (13), and then ζ can be derived from Eqs. (14) or (15). **Fig. 6 presents the**

relative error of ζ with WRL12 equations compared with iterated results of CB05 for various Ri_B with $z/z_0 = 10, 1000, 10^5$ and $kB^{-1} = -0.5, 15, 30$. It shows that the relative error of WRL12 exceeds 20% when Ri_B is small, and exceeds 50% when Ri_B becomes large.

3 Derivation of the new scheme

It can be seen from Fig. 1, Fig. 2 and Fig. 3 that ζ varies with Ri_B , $\log(z/z_0)$ and kB^{-1} with remarkable nonlinearity. Specially, when kB^{-1} is large, $\zeta \sim z_0$ relationship can hardly be approximated by a cubic equation at some Ri_B values (Fig. 2). Correspondingly, when z_0 is large, $\zeta \sim z_{0h}$ also needs a high power series equation to approximate (at least cubic fit is not enough, Fig. 3). In order to reduce the complexity, weakly and strongly stable conditions are treated separately in previous studies (e.g., Launiainen, 1995; Li et al., 2010; WRL12). Analogously, multiple regions are considered for z_0 and z_{0h} for the regression of $\zeta = f(Ri_B, L_{0M}, kB^{-1})$ in this paper. In this way, the complexity of the equations can be reduced and at the same time their accuracy can be maintained. Although the total number of equations is increased due to the division of z_0 and z_{0h} , the calculation efficiency is still enhanced since the logical judgment of the region according to z_0 and z_{0h} values in programme codes takes much less time than iterations. The critical issue here is how to divide the z_0 and z_{0h} regions in a reasonable way to obtain the smallest number of regions but the highest accuracy. For this purpose, the z_0 and z_{0h} are first divided into 13 and 14 sections according to the values of z/z_0 and z_0/z_{0h} , respectively. For z/z_0 , the sections are 10~20, 20~40, 40~80, ..., 10240~20480, 20480~40960 and 40960~ 10^5 ; for z_0/z_{0h} , the sections are 0.607~1, 1~10, 10~100, 100~ 10^3 , $10^3 \sim 10^4$, ..., $10^{11} \sim 10^{12}$ and $10^{12} \sim 1.07 \times 10^{13}$. $z/z_0 \in 10 \sim 20$ and $z_0/z_{0h} \in 10^{12} \sim 1.07 \times 10^{13}$ is the region that needs the highest power series equation to approximate. This region is firstly chosen to find a maximum critical value of ζ_{c1} that can make the regression:

$$\zeta = f(Ri_B, L_{0M}, kB^{-1}) = Ri_B \sum C_{ijk} Ri_B^i L_{0M}^j (L_{0H} - L_{0M})^k \quad (23)$$

be within 5% error when $\zeta \in 0 \sim \zeta_{c1}$. Here i, j , and $k = 0, 1, 2$, and 3 , and $i + j + k \leq 4$. C_{ijk} are the coefficients from regression. It is found that $\zeta_{c1} = 0.33$ meets this criterion. Then some of the z_0 and z_{0h} regions can be merged with each other for the section $\zeta \in 0 \sim 0.33$ and a total of

8 $z_0 - z_{0h}$ regions are left in the $z_0 - z_{0h}$ plane. In other words, the regression error of Eq. (23) can be kept within 5% in any of the 8 regions when $\zeta \in 0 \sim 0.33$ (Table 1). Thus, for these 8 regions, it can be found that with the sections divided by the specified critical values ζ_{cp} (where p is 1,2,3, ... it indicates the section and its maximum value depends on the $z_0 - z_{0h}$ region), the regression error with Eq. (23) can be kept within 5% for $\zeta \leq 0.5$ and 10% or $\zeta > 0.5$. For a given pair of z_0 and z_{0h} , the division by ζ_{cp} can be transformed to Ri_{Bcp} :

$$Ri_{Bcp} = \sum C_{mn} \log^m(L_{0M}) (L_{0H} - L_{0M})^n \quad (24)$$

Here m, n = 0, 1, 2, and $m + n \leq 3$; p is 1,2,3, ..., which indicates the section and its maximum value depends on the $z_0 - z_{0h}$ region. For region 1 and 7, the maximum p is 6, while for other regions it varies between 3 and 5. The coefficients for Eq. (24) are shown in Table 2. The Ri_{Bcp} then cut the 0-2.5 Ri_B range into several sections: section 1 is from 0 to Ri_{Bc1} , section 2 from Ri_{Bc1} to Ri_{Bc2} , and so on. The coefficients for Eq. (23) in each section are given in Tables 3~10.

The procedure to obtain these coefficients are summarized below:

1) Divide z / z_0 into 13 sections: 10~20, 20~40, 40~80, ..., 10240~20480, 20480~40960 and 40960~ 10^5 ; divide z_0 / z_{0h} in to 14 sections: 0.607~1, 1~10, 10~100, 100~ 10^3 , $10^3 \sim 10^4$, ..., $10^{11} \sim 10^{12}$ and $10^{12} \sim 1.07 \times 10^{13}$.

2) Use the region $z / z_0 \in 10 \sim 20$ and $z_0 / z_{0h} \in 10^{12} \sim 1.07 \times 10^{13}$ to find ζ_{c1} . Method: when $\zeta \in 0 \sim \zeta_{c1}$, regression with Eq. (23) is kept within 5% error.

Result: $\zeta_{c1} = 0.33$ found.

3) Use $\zeta_{c1} = 0.33$ to recombine z / z_0 and z_0 / z_{0h} sections defined in step 1.

Method: Variations of combinations of the 13 sections of z / z_0 and 14 sections of z_0 / z_{0h} are tested to minimize the numbers of regions, and regression with Eq. (23) and $\zeta \in 0 \sim 0.33$ is kept within 5% error.

Result: 8 regions found (Table 1)

4) For each of the 8 regions, find $\zeta_{c1}, \zeta_{c2}, \dots, \zeta_{cp}, \dots$

Method: when $\zeta \in 0 \sim \zeta_{c1}$, or $\zeta_{c1} \sim \zeta_{c2}$, ..., or $\zeta_{c(p-1)} \sim \zeta_{cp}$, ..., regression with Eq. (23) is kept within 5% error for $\zeta \leq 0.5$ and 10% error for $\zeta > 0.5$.

Result: $\zeta_{c1}, \zeta_{c2}, \dots, \zeta_{cp}, \dots$, for each region found

5) Transfer $\zeta_{c1}, \zeta_{c2}, \dots, \zeta_{cp}, \dots$, to $Ri_{Bc1}, Ri_{Bc2}, \dots, Ri_{Bcp}, \dots$, with Eq. (24)

Method: for each region, when $Ri_B \in 0 \sim Ri_{Bc1}$, or $Ri_{Bc1} \sim Ri_{Bc2}, \dots$, or

$Ri_{Bc(p-1)} \sim Ri_{Bcp}, \dots$, regression with Eq. (23) is kept within 5% error for $\zeta \leq 0.5$ and 10% error for $\zeta > 0.5$.

Result: coefficients of Eq. (23) and Eq. (24) are derived.

The calculation procedure for a given group of z_0, z_{0h} and Ri_B is that: 1) find the region according to z_0 and z_{0h} with Table 1; 2) Find the section according to the region and Ri_B with Eq. (24) and coefficients in Table 2; and 3) In Table 3-10 find the coefficients for the particular region and section and use Eq. (23) to calculate ζ . Fig. 7 presents the relative error of ζ with new equations compared with iterated results of CB05 for various Ri_B with $z/z_0 = 10, 1000, 10^5$ and $kB^{-1} = -0.5, 15, 30$. With the new equations, the relative error is controlled to be within 10% for the whole range. Specially, when $\zeta \leq 0.5$, the relative error is within 5% since it happens more often in the real conditions (Fig. 8).

4 Comparison of the results from CB05 with 5 steps iteration, WRL12 and the new scheme

The maximum and average relative error of ζ, C_M and C_H calculated from CB05 with 5 steps iteration, WRL12 and the new scheme are shown in Fig. 8, Fig. 9 and Fig. 10 for various ζ with $z/z_0 = 10, 1000, 10^5$ and $kB^{-1} = -0.5, 15, 30$. C_M and C_H are the transfer coefficients for momentum and sensible heat respectively, and:

$$C_M = \frac{k^2}{[\ln(\frac{z}{z_0}) - \psi_m(\zeta) + \psi_m(\frac{z_0}{z}\zeta) + \psi_m^*(\zeta, \frac{z}{z_*})]^2} \quad (25)$$

$$C_H = \frac{k^2}{[\ln(\frac{z}{z_0}) - \psi_m(\zeta) + \psi_m(\frac{z_0}{z}\zeta) + \psi_m^*(\zeta, \frac{z}{z_*})][\ln(\frac{z}{z_{0h}}) - \psi_h(\zeta) + \psi_h(\frac{z_0}{z}\zeta) + \psi_h^*(\zeta, \frac{z}{z_*})]} \quad (26)$$

1 To speed up the calculation, $\psi_{m,h}^*(\zeta, \frac{z}{z_*})$ is not calculated from Eq. (6) but rather from the non-
 2 integral equation proposed by De Ridder (2010):

$$3 \quad \psi_{m,h}^*(\zeta, \frac{z}{z_*}) = \phi_{m,h} \left[\left(1 + \frac{\nu}{\mu z / z_*}\right) \zeta \right] \frac{1}{\lambda} \ln \left(1 + \frac{\lambda}{\mu z / z_*}\right) \exp(-\mu z / z_*) \quad (27)$$

4 where $\lambda = 1.5$, $\mu = \mu_m = 2.59$, $\mu = \mu_h = 0.95$ and $\nu = 0.5$. The relative error for C_M and C_H is
 5 calculated from:

$$6 \quad \Delta C_{M,H} = \frac{|C_{M,H(cal)} - C_{M,H(precise)}|}{C_{M,H(precise)}} \times 100\% \quad (28)$$

7 where $C_{M,H(cal)}$ is calculated with $\zeta_{(cal)}$ from the three different methods, and $C_{M,H(precise)}$ is
 8 calculated with $\zeta_{(precise)}$ from the ultimate iteration of CB05.

9 Maximum error indicates the maximum error for a particular ζ under various z_0 and z_{0h}
 10 conditions, while average error is calculated from

$$11 \quad AverageError(\zeta) = \frac{\int_{-0.5}^{30} \int_{\log(10)}^{\log(10^5)} Error(\zeta) d \log\left(\frac{z}{z_0}\right) d \log\left(\frac{z_0}{z_{0h}}\right)}{\int_{-0.5}^{30} \int_{\log(10)}^{\log(10^5)} d \log\left(\frac{z}{z_0}\right) d \log\left(\frac{z_0}{z_{0h}}\right)} \quad (29)$$

12 Here $Error(\zeta)$ indicates $\Delta\zeta$ or $\Delta C_{M,H}$ at a particular ζ , z_0 and z_{0h} . Although Eq. (28) presents
 13 the form of continuous integral, it is actually calculated discretely with interval 0.035 for
 14 $\log(\frac{z}{z_0})$ and 0.1 for $\log(\frac{z_0}{z_{0h}})$.

15 The results indicate that the maximum $\Delta\zeta$ exceeds 50% when using CB05 with 5 steps iteration
 16 or WRL12, while the averaged $\Delta\zeta$ for the two methods both exceeds 15%. On the contrary,
 17 the maximum $\Delta\zeta$ of the new scheme is always smaller than 5% (when $\zeta \leq 0.5$) and 10%
 18 (when $\zeta > 0.5$), and the average $\Delta\zeta$ is always smaller than 2% in the whole range. The
 19 maximum ΔC_M from CB05 with 5 steps iteration (WRL12) exceeds 50% (40%), and average
 20 ΔC_M exceeds 30% (8%). The maximum ΔC_H from CB05 with 5 steps iteration (WRL12)
 21 exceeds 50% (24%), and average ΔC_H exceeds 18% (6%). Comparatively, the new scheme

controls the maximum ΔC_M (ΔC_H) to be within 12% (9%) and the average ΔC_M (ΔC_H) within 1% (1%). Table 11 summarizes the characteristics of the four methods.

5 Summary and conclusions

Although CB05 provides a way to calculate surface fluxes under stable condition, its practical usage is confined due to the involved iteration process. It has been shown that iteration with 5 steps will result in large calculation errors, especially when z/z_0 is small and kB^{-1} is large, which is common over an urban surface. WRL12 proposed a way to avoid the iteration, but it introduces large error in the calculation procedure so that its calculation accuracy needs be improved. Through dividing the $z_0 - z_{0h}$ plane into 8 regions, the new scheme develops a group of equations with higher accuracy. The calculation error of $\zeta = f(Ri_B, L_{0M}, kB^{-1})$ is always controlled to be within 5% (when $\zeta \leq 0.5$) and 10% (when $\zeta > 0.5$). The calculation procedure is also simple, for a small Ri_B (i.e., $Ri_B < Ri_{Bc1}$), only one time computation of Eq. (23) and (24) will suffice. The maximum computation step is 6 times of Eq. (24) and one time of Eq. (23) when it is in region 1 or 7 and at the same time Ri_B is large (i.e., $Ri_B > Ri_{Bc6}$). Note that the Eq. (24) has only a maximum of 8 elements and a minimum of 4 elements so the calculation is still efficient. The new equations involve a large number of parameters which increase the complexity of coding. However, the effort of coding the new scheme is minimal as compared to its potential gain, which includes the accuracy of the new scheme and the avoidance of iterations. Besides, a compromise can be made between accuracy and complexity. For models that are not interested in high kB^{-1} values, region 1 and 2 (i.e., $10 \leq z/z_0 \leq 10^5$ and $-0.607 \leq z_0/z_{0h} \leq 100$) have provided reasonable coverage (see Garratt, 1992; Launiainen, 1995), and the other 6 regions can be ignored. For example, in WRF model MM5 surface module, $z_{0h} = z_0$ is assumed during the calculation of frictional velocity (Jiménez et al, 2012). While for models that include urban surface effects, it is better to keep all the regions. Further, CB05 probably is not the final solution for the surface flux calculation under stable stratification. The method used to derive non-iterative equations presented here can be used in future studies to transfer the new iterative algorithm to non-iterative equations. Overall, the new equations cover the full range of $-0.5 \leq kB^{-1} \leq 30$, $10 \leq z/z_0 \leq 10^5$ and stable condition (i.e., $0 < Ri_B \leq 2.5$), and maintain high accuracy and efficiency. It is expected that its usage in

climate and weather forecasting models can lead to better performance in surface flux calculation under stable conditions, especially over urban surfaces.

Acknowledgements

This study is supported by China Meteorological Administration under grant GYHY201006024, the National Program on Key Basic Research Project of China (973) under grant 2011CB403501, 2012CB417203 and 2010CB428502, the CAS Strategic Priority Research Program grant XDA05110101, and the National Natural Science Foundation of China under grant 41275022. The first author (YL) is supported by City University of Hong Kong Grant No. 7004002. The authors would like to acknowledge P. A. Jim énez, J. Dudhia, J. F. Gonz ález-Rouco, J. Navarro, J. P. Mont ávez, E. Garc ía-Bustamante, H. Wouters, K. De Ridder and N. P. M. van Lipzig for their two recent papers which made us aware of the deficiency of current surface layer flux schemes. We are grateful to two anonymous reviewers for their careful review and valuable comments, which led to substantial improvement of this manuscript.

References

- Beljaars, A. C. M. and Holtslag, A. A. M.: Flux parameterization over land surfaces for atmospheric models, *J. Appl. Meteorol.*, 30, 327-341, 1991.
- Businger, J. A.: Transfer of momentum and heat in the planetary boundary layer, in *Proceedings of the symposium on the Arctic heat budget and atmospheric circulation*, pp 305-331, 1966.
- Businger, J. A., Wyngaard, J. C., Izumi, Y., and Bardley, E. F.: Flux-profile relationships in the atmospheric surface layer, *J. Atmos. Sci.*, 28, 181-189, 1971.
- Chen, F. and Dudhia, J.: Coupling an advanced land surface-hydrology model with the Penn State-NCAR MM5 modeling system. Part I: Model implementation and sensitivity, *Mon. Wea. Rev.*, 129, 569-585, 2001.
- Cheng, Y. G., and Brutsaert, W.: Flux-profile relationships for wind speed and temperature in the stable atmospheric boundary layer, *Boundary-Layer Meteorol.*, 114, 519-538, 2005.
- De Bruin, H. A. R., Ronda, R. J., and Van De Wiel, B. J. H.: Approximate solutions for the Obukhov length and the surface fluxes in terms of bulk Richardson numbers, *Boundary-Layer Meteorol.*, 95, 145-157, 2000.
- De Ridder K.: Bulk transfer relations for the roughness sublayer, *Boundary-Layer Meteorol.*, 134, 257-267, 2010.
- Dyer, A. J.: The turbulent transport of heat and water vapour in an unstable atmosphere, *Q. J. R. Meteorol. Soc.*, 93, 501-508, 1967.
- Dyer, A. J.: A review of flux-profile relationships, *Boundary-Layer Meteorol.*, 7, 363-372, 1974.
- Fairall, C. W., Bradley, E. F., Rogers, D. P., Edson, J. B., and Young, G. S.: Bulk parameterization of air-sea fluxes for TOGACOARE, *J. Geophys. Res.*, 101, 3747-3764, 1996.
- Fairall, C. W., Bradley, E. F., Hare, J. E., Grachev, A. A., and Edson, J. B.: Bulk parameterization of air-sea fluxes: updates and verification for the COARE algorithm, *J. Clim.*, 16, 571-591, 2003.
- Garratt, J. R.: *The atmospheric boundary layer*. Cambridge University Press, Cambridge, 1992.
- Grachev, A. A. and Fairall, C. W.: Dependence of the Monin-Obukhov stability parameter on the bulk Richardson number over the ocean, *J. Appl. Meteorol.*, 36, 406-414, 1997.

- 1 Grachev A.A., Andreas E.L, Fairall C.W., Guest P.S., and Persson P.O.G.: SHEBA flux-profile
- 2 relationships in the stable atmospheric boundary layer, *Boundary-Layer Meteorol.*, 124,
- 3 315–333, 2007.
- 4 Grachev A. A., Andreas E. L, Fairall C. W., Guest P. S., and Persson P. O. G.: The critical
- 5 Richardson number and limits of applicability of local similarity theory in the stable
- 6 boundary layer, *Boundary-Layer Meteorol.*, 147, 51-82, 2013.
- 7 Guo, X. and Zhang, H.: A performance comparison between nonlinear similarity functions in
- 8 bulk parameterization for very stable conditions, *Environ. Fluid. Mech.*, 7, 239-257, 2007.
- 9 Högström, U.: Review of some basic characteristics of the atmospheric surface layer,
- 10 *Boundary-Layer Meteorol.*, 78, 215-246, 1996.
- 11 Holtslag, A. A. M. and de Bruin, H. A. R.: Applied modelling of the nighttime surface energy
- 12 balance over land, *J. Appl. Meteorol.*, 22, 689-704, 1988.
- 13 Janjić, Z. I.: The step-mountain eta coordinate model: further developments of the convection,
- 14 viscous sublayer and turbulence closure schemes, *Mon. Wea. Rev.*, 122, 927-945, 1994.
- 15 Janjić, Z. I.: The surface layer in the NCEP Eta Model. Eleventh conference on numerical
- 16 weather prediction, Norfolk, VA, 19-23 August 1996. Amer. Meteor. Soc., Boston, MA,
- 17 pp 354-355, 1996.
- 18 Jiménez, P. A., Dudhia, J., González-Rouco, J. F., Navarro, J., Montávez, J. P., and García-
- 19 Bustamante, E.: A revised scheme for the WRF surface layer formulation, *Mon. Wea. Rev.*
- 20 140, 898-918, 2012.
- 21 Launiainen, J.: Derivation of the relationship between the Obukhov stability parameter and the
- 22 bulk Richardson number for flux-profile studies, *Boundary-Layer Meteorol.* 76, 165-179,
- 23 1995.
- 24 Li, Y., Gao, Z., Lenschow, D. H., and Chen, F.: An improved approach for parameterizing
- 25 surface-layer turbulent transfer coefficients in numerical models, *Boundary-Layer*
- 26 *Meteorol.*, 137, 153-165, 2010.
- 27 Louis, J. F.: A parametric model of vertical eddy fluxes in the atmosphere, *Boundary-Layer*
- 28 *Meteorol.*, 17, 187-202, 1979.
- 29 Monin, A. S. and Obukhov, A. M.: Dimensionless characteristics of turbulence in the surface
- 30 layer of the atmosphere, *Trudy. Geofiz. Inst. Akad. Nauk. SSSR*, 24, 163-187, 1954.

1 Nakanishi, M. and Niino, H.: An improved Mellor-Yamada Level-3 model: Its Numerical
2 Stability and Application to a Regional Prediction of Advection Fog, *Boundary-Layer*
3 *Meteorol.*, 119, 397-407, 2006.

4 Paulson, C. A.: The mathematical representation of wind speed and temperature in the unstable
5 atmospheric surface layer, *J. Appl. Meteor.*, 9, 857-861, 1970.

6 Poulos, G. S., Blumen, W., Fritts, D. C., Lundquist, J. K., Sun, J., Burns, S. P., Nappo, C., Banta,
7 R., Newsom, R., Cuxart, J., Terradellas, E., Balsley, B., and Jensen, M.: CASES-99: A
8 Comprehensive Investigation of the Stable Nocturnal Boundary Layer, *Bull. Amer.*
9 *Meteorol. Soc.*, 83, 555–581, 2002.

10 Sanz Rodrigo, J. and Anderson, P.S.: Investigation of the stable atmospheric boundary layer at
11 Halley Antarctica, *Boundary-Layer Meteorol.*, 148, 517-539, 2013.

12 Sarkar, A. and De Ridder, K.: The urban heat island intensity of Paris: a case study based on a
13 simple urban surface parametrization, *Boundary-Layer Meteorol.*, 138, 511–520, 2010.

14 Sharan, M. and Kumar, P.: Estimation of upper bounds for the applicability of non-linear
15 similarity functions for non-dimensional wind and temperature profiles in the surface layer
16 in very stable conditions, *Proc. R. Soc. A.*, 467, 473–494, 2011.

17 Skamarock, W. C., Klemp, J. B., Dudhia, J., Gill, D. O., Barker, D. M., Wang W. and Powers,
18 J. G.: A description of the advanced research WRF version 3, NCAR Technical Note, 2008.

19 Song, Y.: An improvement of the Louis scheme for the surface layer in an atmospheric
20 modelling system, *Boundary-Layer Meteorol.*, 88, 239-254, 1998.

21 Sorbjan, Z.: Gradient-based scales and similarity laws in the stable boundary layer, *Quart. J.*
22 *Roy. Meteorol. Soc.*, 136, 1243–1254, 2010.

23 Sorbjan, Z. and Grachev, A.A.: An evaluation of the flux-gradient relationship in the stable
24 boundary layer, *Boundary-Layer Meteorol.*, 135, 385–405, 2010.

25 Sugawara, H. and Narita, K.: Roughness length for heat over an urban canopy, *Theor. Appl.*
26 *Climatol.*, 95, 291-299, 2009.

27 Wouters, H., De Ridder, K. and van Lipzig, N. P. M.: Comprehensive Parametrization of
28 Surface-Layer Transfer Coefficients for Use in Atmospheric Numerical Models,
29 *Boundary-Layer Meteorol.*, 145, 539-550, 2012.

- 1 Wyngaard, J. C. and Coté O. R.: Cospectral similarity in the atmospheric surface layer, Quart.
- 2 J. Roy. Meteorol. Soc., 98, 590–603, 1972.
- 3 Yang, K., Tamai, N. and Koike, T.: Analytical solution of surface layer similarity equations, J.
- 4 Appl. Meteorol., 40, 1647-1653, 2001.
- 5

1 Table 1. The 8 regions divided by z/z_0 and z_0/z_{0h} values.

Region	z/z_0	z_0/z_{0h}
1	10~160	0.607~100
2	160~10 ⁵	0.607~100
3	10~80	100~10 ⁷
4	80~10 ⁵	100~10 ⁷
5	10~40	10 ⁷ ~10 ¹¹
6	40~10 ⁵	10 ⁷ ~10 ¹¹
7	10~40	10 ¹¹ ~1.07×10 ¹³
8	40~10 ⁵	10 ¹¹ ~1.07×10 ¹³

2

1 Table 2. The coefficients of Eq. (24).

Region		C ₀₀	C ₁₀	C ₂₀	C ₀₁	C ₁₁	C ₂₁	C ₀₂	C ₁₂
1	<i>Ri_{Bc1}</i>	0.3095	-0.2852	0.07955	0.03388	-0.01605	0	0	-1.079E-4
	<i>Ri_{Bc2}</i>	0.3219	-0.2613	0.06753	0.04838	-0.03101	0.003908	-0.00178	0.001165
	<i>Ri_{Bc3}</i>	0.3545	-0.2569	0.06609	0.05837	-0.03934	0.005643	-0.003381	0.002194
	<i>Ri_{Bc4}</i>	0.439	-0.3133	0.08619	0.0893	-0.07112	0.01403	-0.005965	0.003806
	<i>Ri_{Bc5}</i>	0.6887	-0.5375	0.1616	0.1754	-0.1564	0.03489	-0.01277	0.008101
	<i>Ri_{Bc6}</i>	1.706	-1.62	0.5231	0.5124	-0.5026	0.1239	-0.03577	0.02238
2	<i>Ri_{Bc1}</i>	0	0.08606	-0.03048	0.09019	-0.07682	0.01693	0	0
	<i>Ri_{Bc2}</i>	0.2002	0	-0.01589	0	0.00367	0	0.005057	-0.002399
	<i>Ri_{Bc3}</i>	0.4499	0	-0.02397	0.0388	-0.01145	0	0	0
3	<i>Ri_{Bc1}</i>	0.3063	-0.2849	0.07886	0.03104	-0.01423	-5.632E-4	3.684E-6	-2.926E-6
	<i>Ri_{Bc2}</i>	0.3555	-0.3002	0.07855	0.02617	-0.004769	-0.004012	-1.298E-5	9.907E-6
	<i>Ri_{Bc3}</i>	0.5064	-0.4282	0.1229	0.02138	0	-0.00441	0	0
	<i>Ri_{Bc4}</i>	1.638	-1.743	0.5813	0.04471	-0.01874	0	0	0
4	<i>Ri_{Bc1}</i>	0.09742	0	-0.01096	0.04544	-0.03299	0.006383	0	0
	<i>Ri_{Bc2}</i>	0.1768	0	-0.01434	0.03558	-0.02059	0.003327	0	0
	<i>Ri_{Bc3}</i>	0.3636	0	-0.0224	0.04607	-0.02506	0.004152	0	0
5	<i>Ri_{Bc1}</i>	0	0	0	0.04825	-0.01677	-0.004762	-5.212E-4	2.768E-4
	<i>Ri_{Bc2}</i>	0	0	0.08807	0.05219	-0.01822	-0.01245	-8.5E-4	7.516E-4
	<i>Ri_{Bc3}</i>	0	0	0.1219	0.0583	-0.02373	-0.01224	-0.001081	9.539E-4
	<i>Ri_{Bc4}</i>	0	0	0.1609	0.07789	-0.04617	-0.00736	-0.001399	0.001238
	<i>Ri_{Bc5}</i>	0.4437	0	0	0.1349	-0.1388	0.03347	-0.00119	0.001095
6	<i>Ri_{Bc1}</i>	0	0	0	0.05594	-0.03245	0.005037	-3.654E-4	1.135E-4
	<i>Ri_{Bc2}</i>	0.1945	0	0	0.03347	-0.02116	0.002301	0	8.92E-5
	<i>Ri_{Bc3}</i>	0.4288	-0.1436	0.01635	0.03207	-0.01382	0.001571	1.326E-5	-6.424E-6
7	<i>Ri_{Bc1}</i>	0	0	0	0.03681	-0.007664	-0.005619	-1.211E-4	0
	<i>Ri_{Bc2}</i>	0	0	0	0.03655	0	-0.009977	-2.691E-4	1.057E-4
	<i>Ri_{Bc3}</i>	0	0	0	0.03822	0	-0.01036	-3.658E-4	1.769E-4
	<i>Ri_{Bc4}</i>	0	0	0	0.0384	0	-0.009243	-3.629E-4	1.471E-4
	<i>Ri_{Bc5}</i>	0	0	0	0.05616	-0.02275	0	-5.172E-4	2.261E-4
	<i>Ri_{Bc6}</i>	0	0	0	0.1472	-0.1144	0.02796	-0.001218	5.835E-4
8	<i>Ri_{Bc1}</i>	0	0	0	0.05139	-0.02991	0.004664	-2.135E-4	6.535E-5
	<i>Ri_{Bc2}</i>	0	0	0	0.04919	-0.0197	0.002011	-3.325E-4	7.974E-5
	<i>Ri_{Bc3}</i>	0.5775	-0.2236	0.03477	0.03805	-0.01617	0.00177	-2.191E-5	1.067E-5

2

Table 3. The coefficients of Eq. (23) for Region1.

	Region 1						
	Section 1	Section 2	Section 3	Section 4	Section 5	Section 6	Section 7
C ₀₀₀	-1.134	0	0	0	0	0	0
C ₁₀₀	31.1	86.35	-280.4	0	0	-17.32	-6.343
C ₂₀₀	-71.16	0	3235	0	0	8.773	7.66
C ₃₀₀	227.4	0	-6165	0	0	0	-0.7661
C ₀₀₁	-0.2094	-11.53	-10.64	0	0	0	0.0125
C ₁₀₁	3.293	194.9	193.8	0	1.113	0	-2.203
C ₂₀₁	-20.11	-975.4	-1194	-12.37	-97.56	0	0.8896
C ₃₀₁	14.42	1472	2161	0	159.4	0	-0.1273
C ₀₀₂	0.1476	-2.535	-4.603	0	0	1.919	-0.00827
C ₁₀₂	-0.07325	28.24	52.02	11.99	16.33	0	0.3327
C ₂₀₂	0.5627	-61.13	-110.7	-15.63	-25.67	0.2679	-0.04613
C ₀₀₃	-0.01178	-0.2378	-0.5367	-0.3157	-0.6447	-0.2892	0
C ₁₀₃	0.0218	0.7405	1.503	0.2948	0.9718	0	-0.04968
C ₀₁₀	1.405	13.6	30.26	0	6.821	10.27	7.513
C ₁₁₀	-32.47	-316.2	-314.9	0	-57.13	0	0
C ₂₁₀	46.59	1067	186	-108.1	227.3	0	-4.799
C ₃₁₀	-38.25	-1494	0	317.8	-244	0	0.5598
C ₀₁₁	-0.2286	8.023	9.038	0	0.9287	-3.457	-1.612
C ₁₁₁	-1.097	-91.31	-87.06	-12.52	-17.88	-1.617	0
C ₂₁₁	-0.3394	213.7	198.6	0	34.41	0	0
C ₀₁₂	0	1.035	1.529	0	0.319	-0.07536	0.4666
C ₁₁₂	0	-5.072	-7.439	-1.025	-2.452	0	0.0605
C ₀₁₃	0	0.03622	0.07369	0.04669	0.08583	0.05146	-0.01808
C ₀₂₀	0	-4.699	-10.71	-1.896	-2.195	-3.108	0
C ₁₂₀	10.71	97.46	122.1	28.39	22.21	7.948	2.442
C ₂₂₀	0	-152.4	-76.91	-14.19	-31.44	-2.985	0.1584
C ₀₂₁	0	-1.704	-2.035	0	-0.1355	0.8751	0
C ₁₂₁	0	9.069	8.248	2.214	1.976	0.3139	-0.04377
C ₀₂₂	0	-0.09576	-0.1263	-0.01472	-0.04636	-0.05131	-0.0694
C ₀₃₀	-0.007485	0.4446	1.015	0.3069	0.1708	0.2598	-0.1675
C ₁₃₀	-0.9671	-7.991	-10.96	-3.635	-1.623	-0.8513	-0.2181
C ₀₃₁	0.003402	0.1138	0.1426	-0.008769	0	-0.05427	0.05052

1 Table 4. Similar to Table 3, but for Region2.

2

	Region 2			
	Section 1	Section 2	Section 3	Section 4
C ₀₀₀	0	0	0	0
C ₁₀₀	0	0	41.53	0
C ₂₀₀	0	0	0	0
C ₃₀₀	0	0	0	0
C ₀₀₁	0	0	-1.616	-2.57
C ₁₀₁	0	-12.35	0	-2.91
C ₂₀₁	0	0	0	0
C ₃₀₁	0	0	0	0
C ₀₀₂	0	0	0	0.874
C ₁₀₂	0	0.5183	0	0.3377
C ₂₀₂	0	0	0	0
C ₀₀₃	0	0	0	-0.002092
C ₁₀₃	0	0	0	-0.01343
C ₀₁₀	0.9996	0.8247	0	7.453
C ₁₁₀	0	0	15.82	5.4
C ₂₁₀	56.57	112.5	-27.37	-1.623
C ₃₁₀	0	0	0	0.1999
C ₀₁₁	-0.1456	-0.09054	0	0
C ₁₁₁	0	0	0	0.4753
C ₂₁₁	-12.1	-2.249	0	0
C ₀₁₂	0	0.01653	0	-0.2047
C ₁₁₂	0.1303	0	0.02288	-0.02581
C ₀₁₃	0	0	0	0
C ₀₂₀	0	0	0.1062	-0.9043
C ₁₂₀	0.295	0.8326	-0.9992	-0.3386
C ₂₂₀	0	-9.554	1.56	0.04556
C ₀₂₁	0.005508	0	0	0.04682
C ₁₂₁	-0.0359	0.07022	0	-0.01924
C ₀₂₂	4.067E-4	-0.001333	0	0.01217
C ₀₃₀	0	0	0	0.03944
C ₁₃₀	0	0	0	0.006516
C ₀₃₁	0	0	0	-0.003571

3

1 Table 5. Similar to Table 3, but for Region 3.

2

	Region 3				
	Section 1	Section 2	Section 3	Section 4	Section 5
C ₀₀₀	2.001	0	-68.85	-1.514	0
C ₁₀₀	-0.7876	0	756.9	0	0
C ₂₀₀	0	0	-1100	0	0
C ₃₀₀	60.42	368.9	0	19.63	0
C ₀₀₁	-0.1401	3.514	0	0.559	0
C ₁₀₁	-0.1085	-8.524	-30.13	0	0
C ₂₀₁	-2.065	-18.05	86.99	0	0
C ₃₀₁	-2.98	-4.852	5.71	-2.424	0
C ₀₀₂	0.01334	0.08174	0.7274	-0.002248	0
C ₁₀₂	0.0213	0.5791	-2.554	0	0
C ₂₀₂	0.1963	0.1207	-0.2169	0.1259	0
C ₀₀₃	-3.704E-4	-0.007021	0.01587	8.267E-4	2.413E-4
C ₁₀₃	-0.002957	0	0.003912	-0.004141	7.107E-5
C ₀₁₀	-1.442	1.207	76.25	-8.751	0
C ₁₁₀	1.047	-31.68	-874.1	51.96	1.905
C ₂₁₀	0	32.78	1636	-76.51	-1.761
C ₃₁₀	0	-25.65	-1040	27.69	0.3658
C ₀₁₁	0	-2.096	4.942	-1.349	-0.05227
C ₁₁₁	0	2.222	-17.32	1.297	0
C ₂₁₁	-1.121	0.3871	14.97	-0.09621	0
C ₀₁₂	0	-0.004486	-0.09096	0	0
C ₁₁₂	0.0273	-0.06669	0.2281	0	0
C ₀₁₃	0	0.001086	-0.002971	2.192E-4	0
C ₀₂₀	0.6868	-0.07632	-21.66	3.734	2.165
C ₁₂₀	0	14.32	232.4	-6.438	0.6139
C ₂₂₀	3.82	2.353	-224.1	6.284	-0.1166
C ₀₂₁	-0.01898	0.3396	-1.724	0.2422	-0.07307
C ₁₂₁	-0.1228	-0.3281	3.144	-0.2272	0.005656
C ₀₂₂	2.845E-4	-3.6E-4	-4.477E-4	0	0
C ₀₃₀	-0.06543	0	1.875	-0.4111	-0.3134
C ₁₃₀	0.1469	-1.505	-18.02	0.2556	0
C ₀₃₁	0.00179	-0.01529	0.1523	-0.009961	0.008105

3

1 Table 6. Similar to Table 3, but for Region 4.

2

	Region 4			
	Section 1	Section 2	Section 3	Section 4
C ₀₀₀	0	-3.528	0	0
C ₁₀₀	0	0	0	0
C ₂₀₀	0	0	0	-8.306
C ₃₀₀	0	0	0	1.212
C ₀₀₁	0	-0.2511	-1.018	0
C ₁₀₁	0	0	0	0
C ₂₀₁	-6.267	-10.06	0	0
C ₃₀₁	0	0	0	0
C ₀₀₂	0	0	0	0
C ₁₀₂	0.09808	0.1809	0	0.0279
C ₂₀₂	0	0	0	0
C ₀₀₃	0	0	6.74E-5	6.853E-4
C ₁₀₃	0	0	0.001341	-9.314E-4
C ₀₁₀	0.5961	1.375	-2.404	5.253
C ₁₁₀	0	2.951	41.12	7.626
C ₂₁₀	18.49	68.09	-48.05	-0.2889
C ₃₁₀	34.53	0	24.94	0.06073
C ₀₁₁	-0.0845	0	-0.06671	-0.3959
C ₁₁₁	-0.5106	-1.361	0	-0.07098
C ₂₁₁	-0.3543	0	-0.1319	0.003821
C ₀₁₂	0.004555	0.003711	0.006818	0
C ₁₁₂	0	0	0	0
C ₀₁₃	-9.402E-5	0	-1.788E-4	0
C ₀₂₀	0.05628	-0.02359	0.5172	-0.5006
C ₁₂₀	0.8075	0.305	-4.023	-0.7376
C ₂₂₀	0	-3.765	2.074	0
C ₀₂₁	0	-0.001535	0	0.04853
C ₁₂₁	0.01631	0.07098	0	0.002956
C ₀₂₂	-3.8E-5	-2.577E-4	0	0
C ₀₃₀	-0.00189	0	-0.0192	0.01968
C ₁₃₀	-0.03755	0	0.125	0.025
C ₀₃₁	5.177E-5	0	0	-0.001897

3

1 Table 7. Similar to Table 3, but for Region 5.

2

	Region 5					
	Section 1	Section 2	Section 3	Section 4	Section 5	Section 6
C ₀₀₀	0	0	-207.7	-587.1	0	0
C ₁₀₀	0	77.11	880	2726	7.886	0
C ₂₀₀	-2.541	-201.2	-1550	-3759	-0.5889	0
C ₃₀₀	25.22	386.1	2201	1605	0	0
C ₀₀₁	-0.03201	-0.6831	0	-9.376	-0.4057	0
C ₁₀₁	0.1159	0	11.61	-4.513	0	0
C ₂₀₁	-0.5745	-7.571	-96.51	70.55	-0.5218	0
C ₃₀₁	-0.8502	-8.978	0	-58.16	0	0
C ₀₀₂	0.00208	0.07136	0.5093	0.1711	0.01745	0
C ₁₀₂	-0.001668	0	0.8873	-0.9373	-0.01349	0
C ₂₀₂	0.03737	0.3442	0.2868	1.132	0.01468	0
C ₀₀₃	-1.828E-5	0	-0.001909	-0.006865	0	0
C ₁₀₃	-3.967E-4	-0.003421	-0.004313	-0.001126	0	0
C ₀₁₀	0.4298	0	189.4	286.9	0	0
C ₁₁₀	-0.03339	-31.72	-543.8	-903.7	0	0
C ₂₁₀	0.05692	2.558	324	407.6	0	0
C ₃₁₀	0	0	-80.25	260.2	0	0.08919
C ₀₁₁	-0.0233	0	-5.403	0	0	0
C ₁₁₁	0	2.695	14.95	14.82	0.2908	0
C ₂₁₁	-0.3158	-2.449	-1.706	-26.07	0.1992	0
C ₀₁₂	0	-0.05044	-0.4221	0.01062	-0.003177	0
C ₁₁₂	0.007595	0.05465	0.164	0.2099	-0.00933	0
C ₀₁₃	0	-6.869E-5	-0.00111	9.863E-4	0	0
C ₀₂₀	0	0.3612	-53.83	-44.24	0.7321	2.053
C ₁₂₀	0	0	89.42	98.98	2.304	0.2534
C ₂₂₀	1.793	18.63	34.6	22.67	-2.456	-0.2585
C ₀₂₁	0.00249	0.1236	2.704	-0.01096	-0.09448	-0.0338
C ₁₂₁	-0.05666	-0.837	-4.573	-1.67	0.007636	0.004269
C ₀₂₂	0	0.008316	0.0718	-0.01056	0.002124	0
C ₀₃₀	0	-0.06987	4.95	2.138	0	-0.3116
C ₁₃₀	0.129	0.8756	-3.112	-4.604	0	0.1241
C ₀₃₁	0	-0.01959	-0.3287	0.054	0	0

3

1 Table 8. Similar to Table 3, but for Region 6.

2

	Region 6			
	Section 1	Section 2	Section 3	Section 4
C ₀₀₀	0	0.4383	0	-6.744
C ₁₀₀	-7.864	0	-41.74	8.8
C ₂₀₀	0	0	177	-13.03
C ₃₀₀	0	0	-118.2	2.203
C ₀₀₁	-0.02699	0	0	-0.1139
C ₁₀₁	0.7414	-4.81	-4.006	-0.06103
C ₂₀₁	-1.114	5.094	-0.5102	0.2406
C ₃₀₁	0	-1.159	0	-0.04635
C ₀₀₂	0	0.04547	0	0.01341
C ₁₀₂	0	0	0.0567	-0.002749
C ₂₀₂	0	-0.1233	0.1868	5.316E-6
C ₀₀₃	0	-5.595E-4	0.002457	-1.434E-4
C ₁₀₃	1.281E-4	0.002459	-0.006455	0
C ₀₁₀	0.244	0	0	6.511
C ₁₁₀	1.743	0	27.45	6.369
C ₂₁₀	4.749	44.44	-17.37	-0.175
C ₃₁₀	11.28	0	-7.74	0.03419
C ₀₁₁	0	0	0	-0.3147
C ₁₁₁	-0.3093	0	0	-0.06781
C ₂₁₁	-0.2208	-0.6068	0.0117	-2.026E-4
C ₀₁₂	0	-0.005459	-0.01576	0.002444
C ₁₁₂	0.003674	0	0.02102	2.616E-4
C ₀₁₃	0	0	-1.975E-5	-5.149E-6
C ₀₂₀	0.04168	0	-0.1563	-0.6219
C ₁₂₀	0.4341	0.9983	-2.085	-0.598
C ₂₂₀	0.6518	-2.874	0.3443	0.002868
C ₀₂₁	-0.00208	-0.00152	0.03278	0.03359
C ₁₂₁	0	0.01501	-0.0325	0.003178
C ₀₂₂	2.895E-5	3.541E-4	5.167E-4	-1.423E-4
C ₀₃₀	0	0.006587	0.008163	0.02407
C ₁₃₀	-0.01307	-0.04253	0.0854	0.0188
C ₀₃₁	1.425E-5	-3.659E-4	-0.001602	-0.001167

3

1 Table 9. Similar to Table 3, but for Region 7.

2

	Region 7						
	Section 1	Section 2	Section 3	Section 4	Section 5	Section 6	Section 7
C ₀₀₀	-1.412	-4.502	-104.2	542.4	178.4	0	0
C ₁₀₀	6.658	40.44	136.3	-1845	158.8	0	0
C ₂₀₀	-5.68	37.42	233.3	2157	-480.9	0	0
C ₃₀₀	11.9	0	0	0	0	0	0
C ₀₀₁	0.1285	0.3067	13.8	-3.691	-31.49	0	0
C ₁₀₁	-0.111	-5.444	-37.21	3.33	47.56	0	0
C ₂₀₁	-0.2095	2.053	10.33	-45.62	-4.153	0	0
C ₃₀₁	-0.3181	0	0	0	0	0	0
C ₀₀₂	-0.004693	0.05302	-0.1157	0.1434	0.3998	0	0
C ₁₀₂	0.004467	0	0.5542	0.4557	-0.8692	0	0
C ₂₀₂	0.01324	-0.01586	-0.2568	0.08936	0.2504	0	0
C ₀₀₃	6.64E-5	0	0	0	0	0	0
C ₁₀₃	-2.023E-4	0	0	0	0	0	0
C ₀₁₀	0.7122	1.663	16.56	-263.7	-37.94	0	0
C ₁₁₀	-4.599	-28.1	0	677.7	-147.8	20.56	0
C ₂₁₀	2.705	-11.02	-114.4	-644.2	144.7	-13.42	0
C ₃₁₀	0	0	0	0	0	3.002	0
C ₀₁₁	-0.04962	0.1172	-3.238	4.44	9.904	-0.5254	0.06758
C ₁₁₁	0.01147	1.979	7.578	-3.037	-7.914	0	0
C ₂₁₁	-0.1621	-0.7285	0	10.93	-2.224	0	0.003671
C ₀₁₂	0.001459	-0.0293	0	-0.08875	-0.1235	0	0
C ₁₁₂	0.003514	0.01334	-0.06568	-0.1436	0.1631	0	-6.967E-4
C ₀₁₃	-2.01E-5	0	0	0	0	2.282E-4	0
C ₀₂₀	0.003692	-0.4475	0	32.93	0	0	0
C ₁₂₀	1.299	5.193	-0.1495	-56.58	23.51	-2.349	0.6983
C ₂₂₀	0.6516	5.593	18.12	53.14	-2.645	0.628	-0.1455
C ₀₂₁	0	-0.009728	0.167	-0.951	-0.7278	0.2176	0
C ₁₂₁	-0.03414	-0.3375	-0.6387	0	-0.1801	0.02067	0
C ₀₂₂	2.84E-5	0.00347	0.00428	0.02119	0.008599	-0.005396	-4.282E-4
C ₀₃₀	6.293E-4	0	0	0	0	-0.4148	0
C ₁₃₀	-0.02559	0	0	0	0	0.02245	0
C ₀₃₁	0	0	0	0	0	0.01163	0

3

1 Table 10. Similar to Table 3, but for Region 8.

2

	Region 8			
	Section 1	Section 2	Section 3	Section 4
C ₀₀₀	-3.13	-49.55	0	0
C ₁₀₀	5.26	97.14	0	0
C ₂₀₀	-29.85	352.5	10.72	0
C ₃₀₀	57.04	-573.4	0	0
C ₀₀₁	0.2176	2.052	0	0
C ₁₀₁	-0.00898	-21.41	0	0
C ₂₀₁	-1.756	13.12	0	0
C ₃₀₁	-1.663	20.82	-1.354	0
C ₀₀₂	-0.007271	0.1357	-0.06227	0
C ₁₀₂	0.0304	0.238	0	-0.01477
C ₂₀₂	0.05349	-0.7316	0.08799	-0.001292
C ₀₀₃	8.978E-5	-0.003367	0.002359	0
C ₁₀₃	-6.252E-4	0.006023	-0.002387	3.921E-4
C ₀₁₀	0.9846	14.57	-0.2492	0
C ₁₁₀	-1.011	0	19.79	0
C ₂₁₀	14.45	0	-18.86	-0.8522
C ₃₁₀	4.433	-54.39	9.463	0.1065
C ₀₁₁	-0.05083	-0.8911	0	0
C ₁₁₁	-0.2604	1.478	0	0.374
C ₂₁₁	-0.2977	2.13	-0.3291	0.004036
C ₀₁₂	0.001361	-9.36E-4	0	0.002528
C ₁₁₂	0.00375	-0.04272	0.01369	-0.006853
C ₀₁₃	-1.464E-5	1.939E-4	-2.41E-4	-8.747E-5
C ₀₂₀	-0.004659	-1.165	0	0
C ₁₂₀	0.6393	0	-1.689	-0.4307
C ₂₂₀	0	-3.616	1.036	0.01469
C ₀₂₁	0	0.06747	0.00194	0.001642
C ₁₂₁	0	0.01581	-0.02897	0
C ₀₂₂	0	-3.126E-4	8.316E-4	0
C ₀₃₀	8.014E-4	0.03485	0.01694	0
C ₁₃₀	-0.01934	0	0.06734	0.01348
C ₀₃₁	0	-0.001713	-0.001447	0

3

4

Table 11. Summarization of the characteristics of the four methods. Calculation time is the time each method needs for computing ζ from Ri_B , z_0 and z_{0h} in the range $0 < Ri_B \leq 2.5$, $10 \leq z/z_0 \leq 10^5$ and $-0.5 \leq \log(z_0/z_{0h}) \leq 30$ with the interval of 0.01 for Ri_B , 0.035 for $\log(z/z_0)$ and 0.1 for $\log(z_0/z_{0h})$. The calculation is performed on a desktop computer with an Intel Core i5 processor, and note that the calculation time can vary with different computer.

Method	Calculation time	Maximum $\Delta\zeta$	Average $\Delta\zeta$	Characteristics and suggestion
CB05 with ultimate iteration	6260 s	N/A	N/A	Current optimal method, but with high computational cost. Use this method when computing power is not an issue.
CB05 with 5 steps iteration	3960 s	exceeds 50%	exceeds 15%	Lower computational cost, but add more uncertainty in the calculation procedure of CB05.
WRL12	261 s	exceeds 50%	exceeds 15%	Much lower computational cost, but add more uncertainty in the calculation procedure of CB05.
New equations	549 s	smaller than 5% (when $\zeta \leq 0.5$) and 10% (when $\zeta > 0.5$)	smaller than 2%	Low computational cost, error in the calculation procedure of CB05 is controlled within 10%. Use this method to have an optimal compromise between accuracy and computational cost.

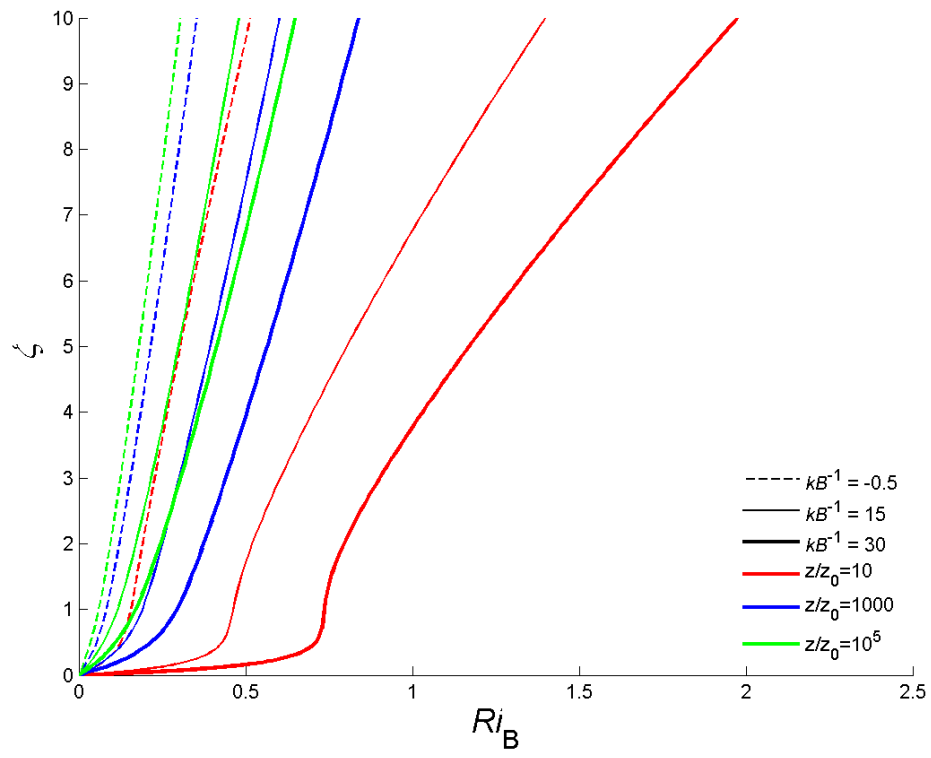
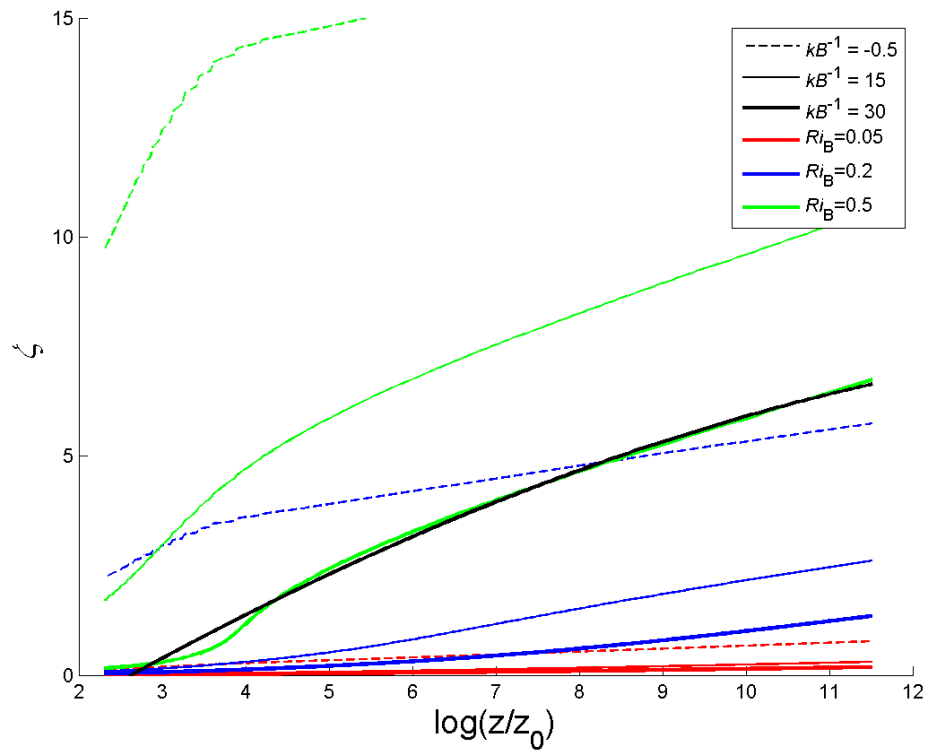


Figure 1. The relationship between Ri_B and ζ from the precise results of CB05

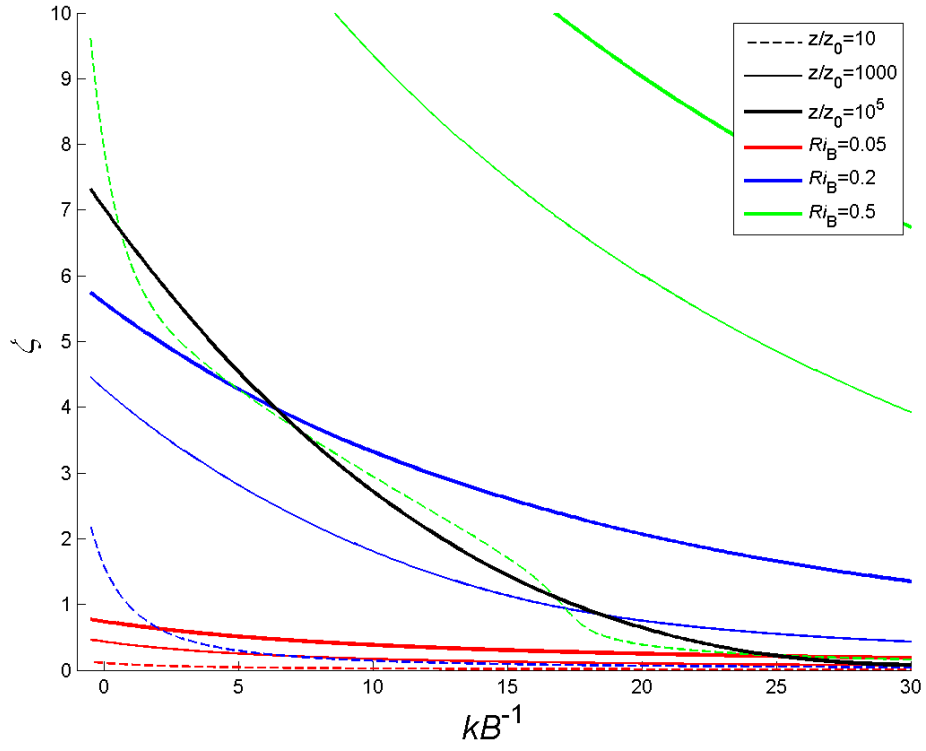


1

2 Figure 2. The relationship between $\log(z/z_0)$ and ζ from the precise results of CB05. Black line

3 indicates the cubic fit of curve $k_B^{-1}=30$ and $Ri_B=0.5$ with least square method.

4



1

2 Figure 3. The relationship between $\log(z/z_{0h})$ (i.e., kB^{-1}) and ζ from the precise results of CB05.

3 Black line indicates the cubic fit of curve $z/z_0=10$ and $Ri_B=0.5$ with least square method.

4

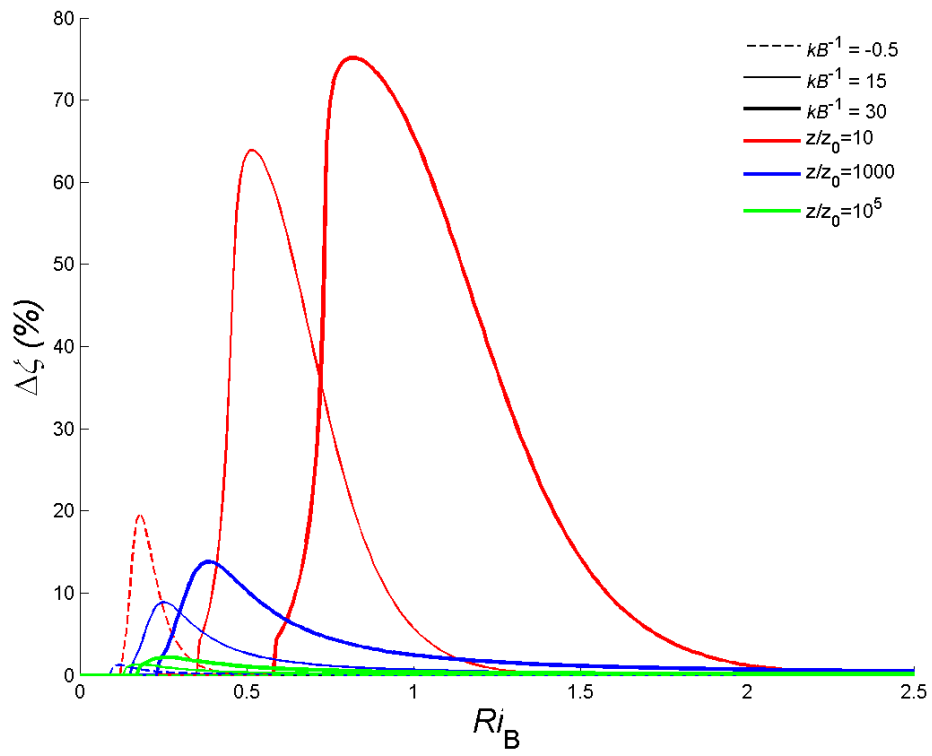


Figure 4. Relative error after 5 steps of iteration with CB05 equations under certain z_0 and z_{0h} conditions.

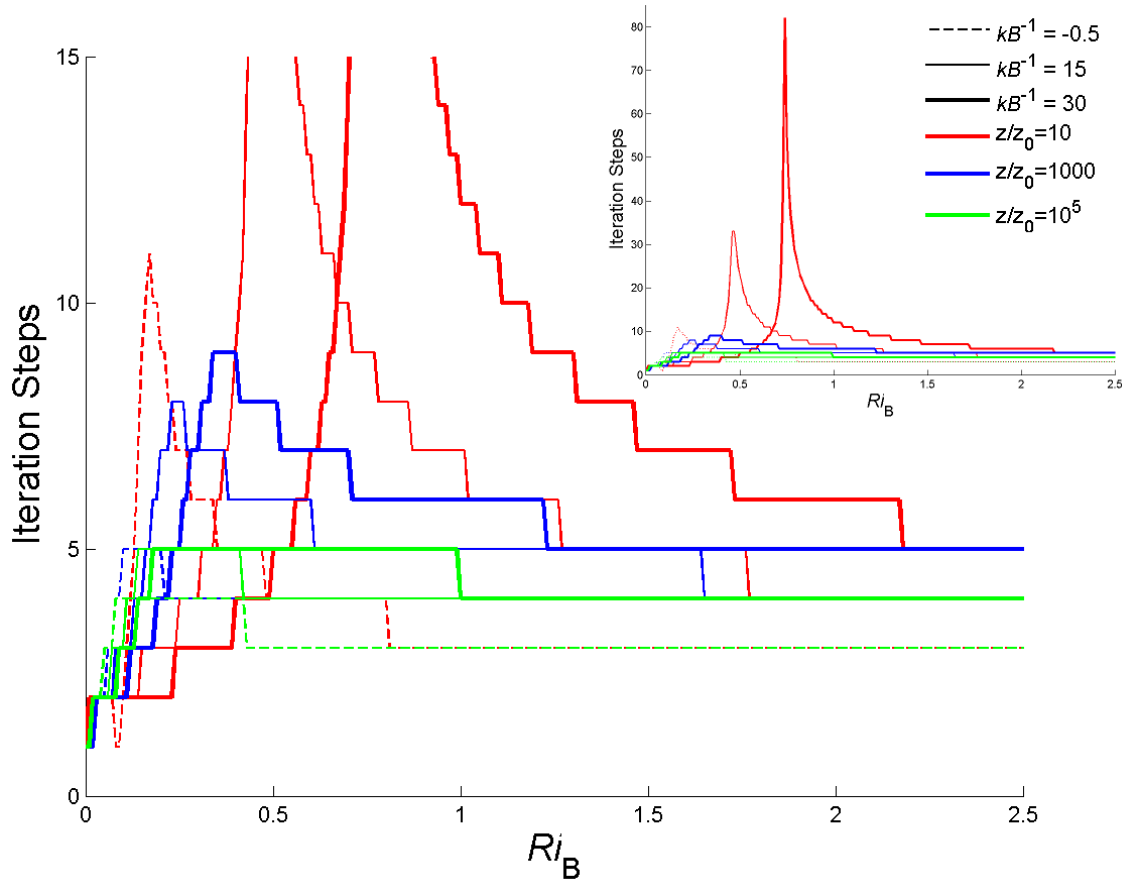
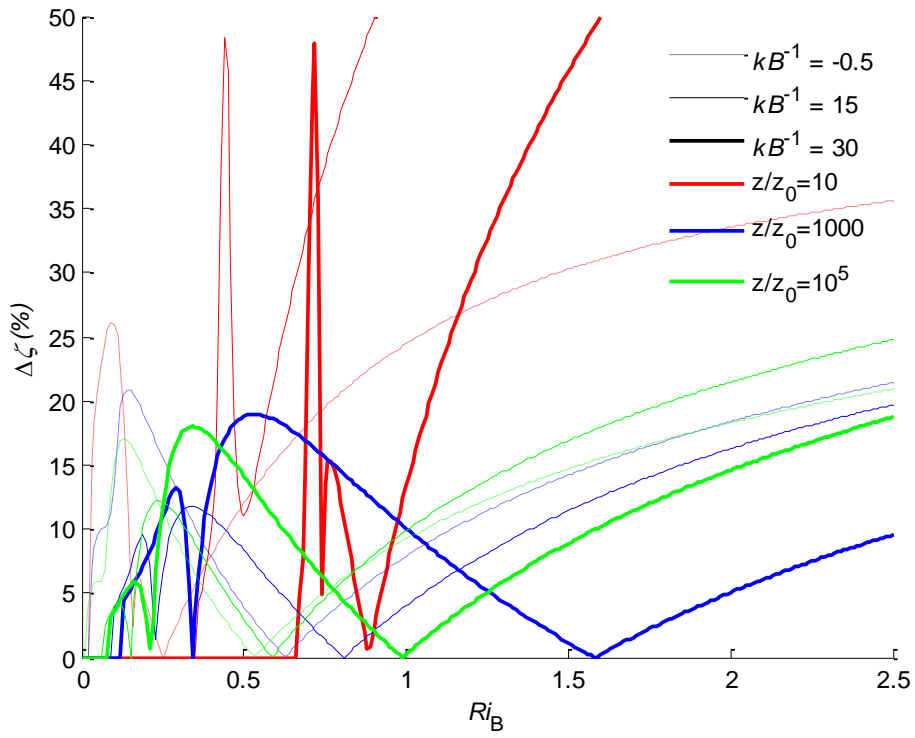


Figure 5. Steps needed to converge into 5% relative error with CB05 equations under certain z_0 and z_{0h} conditions. The inset shows the whole perspective.



1

2 Figure 6. Relative error with WRL12 equations.

3

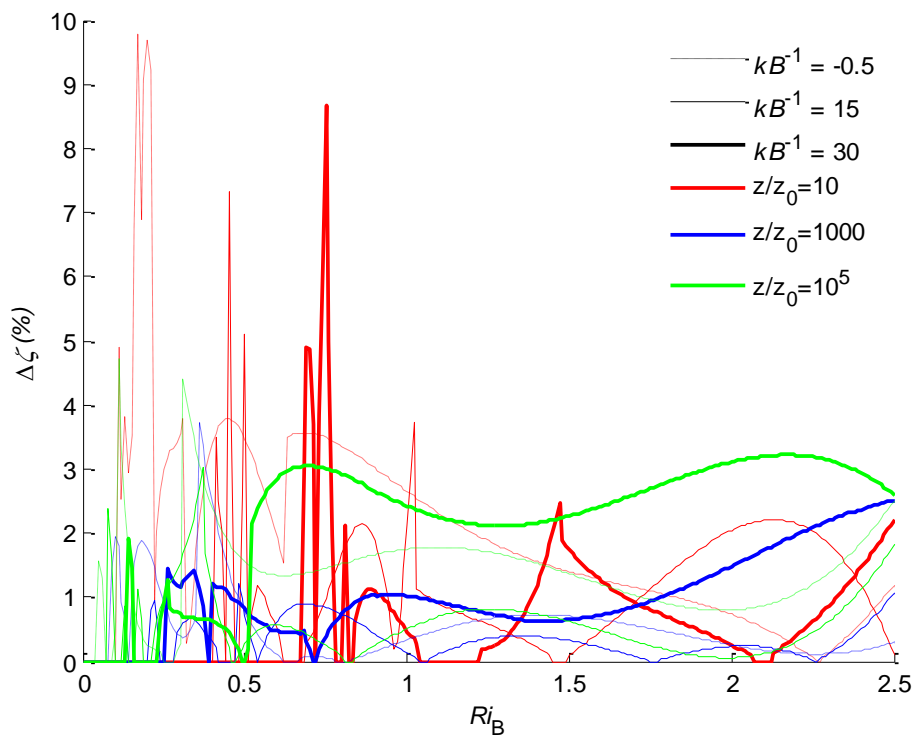


Figure 7. Relative error with new equations.

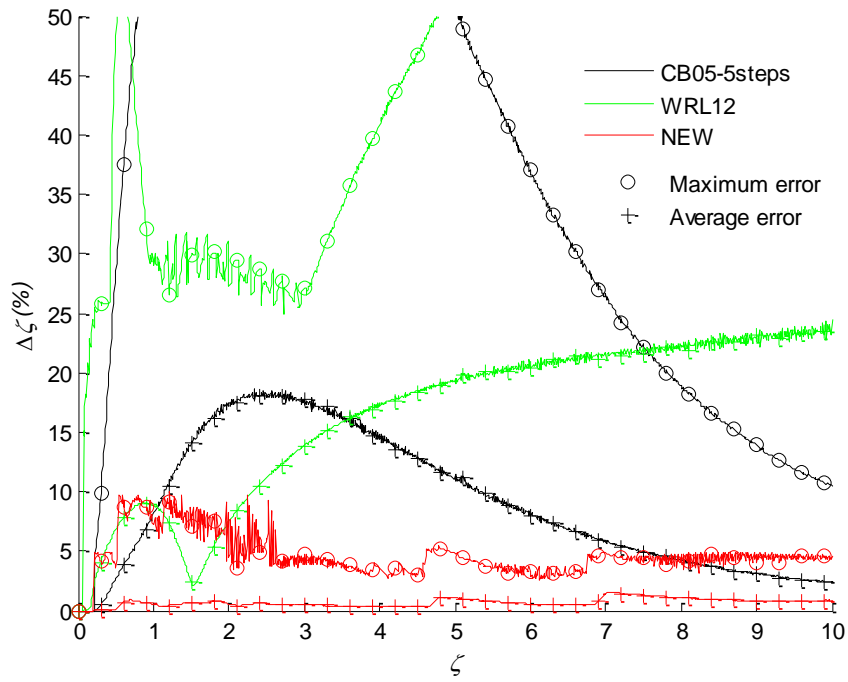


Figure 8. Maximum (circles) and average (crosses) relative error of ζ for CB05 with 5 steps iteration (black lines), WRL12 (green lines) and the new scheme (red lines). Errors larger than 50% are not shown.

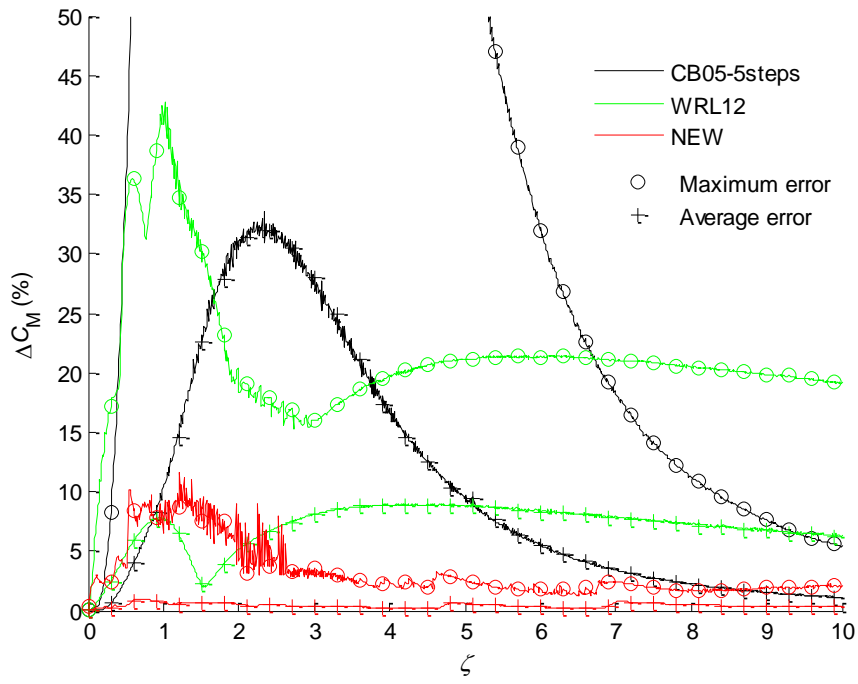


Figure 9. Similar to Figure 8 but for C_M .

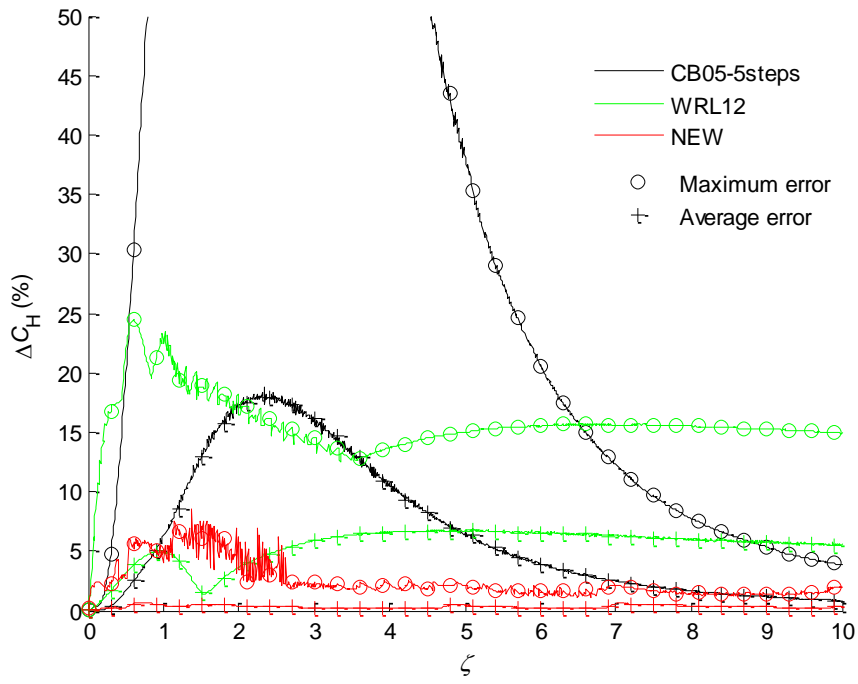


Figure 10. Similar to Figure 8 but for C_H .